Original papers

Granular Matter 4, 39–44 © Springer-Verlag 2002
DOI 10.1007/s10035-002-0105-7

Dynamics of a gas bubble rising through a thin immersed layer of granular material: an experimental study

L. Gostiaux, H. Gayvallet, J.-C. Géminard

Abstract Packings of non-cohesive grains, immersed in a fluid, differ significantly from *classical* porous media as the grains, subjected to stresses and flows, can move within the sample, changing then the local properties of the material. We study experimentally the conditions for a gas to pass through a layer of immersed granular material. Above a threshold pressure, which depends mainly on the grains size and on the surface free energy of the liquid-gas interface, the gas creates a channel within the whole thickness of the layer.

Keywords Granular material, Granular flow, Porous material, Non-newtonian fluid

1 Introduction

Granular materials exhibit complex and puzzling phenomena. Understanding the behavior of materials constituted from a large number of non-cohesive grains is of great practical interest as granular materials are involved in many industrial processes as well as in many natural phenomena. The complex static and flow properties of dry granular materials (i.e. the grains are in vacuum or the interstitial fluid is a gas, such as air) have been extensively studied during the last decades [1]. Immersed granular materials (i.e. the interstitial fluid is a liquid, such as water) also focus attention as they appear in many geophysical or industrial situations. For instance, sand ripples, that form on the ocean floor, play an important role in the transport of sediments [2]. The mixing of a powder and a fluid is obviously a daily operation of the processing industry.

The strength of granular matter is an important macroscopic property. Under many circumstances, a granular material at rest can sustain a load (i.e. it behaves like a solid). Under different circumstances, they flow like liquids. Both immersed and dry granular materials submitted to a shear stress exhibit frictional properties like solids [3]. Vibrated granular layers exhibit surface waves like liquids [4].

We are concerned here with a practical situation: A large volume of gas is trapped underneath an immersed layer of granular material. We study the conditions under which the gas can escape the system. In the everyday life, if one pours liquid at the surface of a powder, a large amount of air can remain trapped within the granular material. This is the case when one tries to prepare a drug by pouring first the powder and then the water, or to mix pancake mix by adding water to flour. In nature, this situation corresponds, for instance, to gas produced by decomposition of organic materials that remains trapped underneath a layer of sediments.

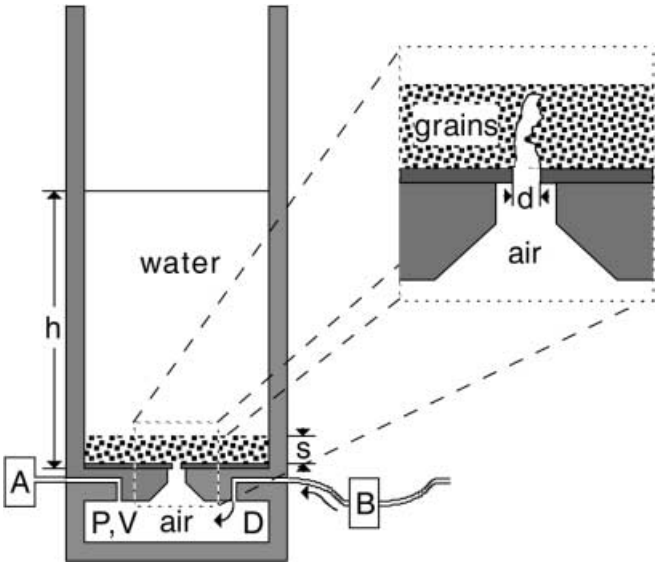

Fig. 1. Experimental setup

2 Experimental setup

The principle of the experiment is the following: An immersed layer of grains rests on a horizontal rough plate. Below, a chamber contains a large volume of gas. The two parts of the system are connected by a hole. We increase and measure the pressure in the chamber and observe the bubbles that go through the granular layer.

The experimental setup (Fig. 1) consists in a vertical plexiglass tube (inner diameter 90 mm, height 300 mm) divided in two parts along its length. The granular layer (thickness s) lies at the bottom of the upper part. The grains are immersed in water (height h, ranging from 0 to 250 mm). The lower part of the cylinder forms a chamber (volume $V = 63$ cm^3) which is filled with air. We measure the pressure P in the chamber (relative to the outside pressure) with the help of a pressure transducer (A) (OMEGA

Received: 23 January 2002

L. Gostiaux, H. Gayvallet, J.-C. Géminard (✉)
Laboratoire de Physique de l'E.N.S. de Lyon,
46 Allée d'Italie, 69364 Lyon Cedex, France
e-mail: geminard@ens-lyon.fr

PX170). A mass flow controller (B) (EL-Flow F201C) introduces air in the chamber at constant rate D (0.2 to 4.3 mg/s). The two parts of the system are connected by a channel (diameter 6 mm), ended by a hole (diameter d, ranging from 1 to 3 mm). A PC computer, equipped with an acquisition board (Data Translation DT300), makes possible to control the mass flow, and to record the pressure signal. The accuracy of the pressure measurements is 0.1 Pa with a time resolution of about 0.1 ms. In addition, we digitize images of the granular layer with a video frame grabber (Data Translation DT3155).

The granular materials consist of monodisperse spherical glass beads (diameters 112 ± 12, 225 ± 25, or 450 ± 50 μm). We use clean grains (without any specific surface treatment) immersed in water, except when specified.

The preparation of the system previous to each of the experiments is the following: We introduce initially a given amount of granular material in the upper part of the cylinder. We afterwards pour a volume of water large enough to immerse all the grains. During this preparation procedure, in order to avoid water or grains to flow down through the hole, a small mass flow of air helps in maintaining an overpressure in the chamber. We obtain a flat free surface of the granular layer by stirring the mixture with a rod, breaking the flow, and waiting for a complete deposition of the grains by slow sedimentation. We then impose a given mass flow D, observe emission of bubbles through the layer and simultaneously record the pressure signal.

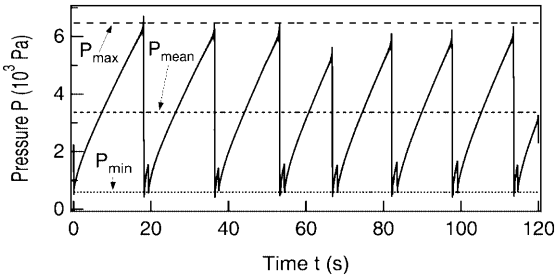

Fig. 2. Typical behavior of the pressure P vs. time t. $P_{min} = 130$ Pa, $P_{moy} = 2930$ Pa, and $P_{max} = 5900$ Pa. ($D = 0.22$ mg/s, $s = 13$ mm, $h = 40$ mm, $d = 2$ mm, beads 112 μm)

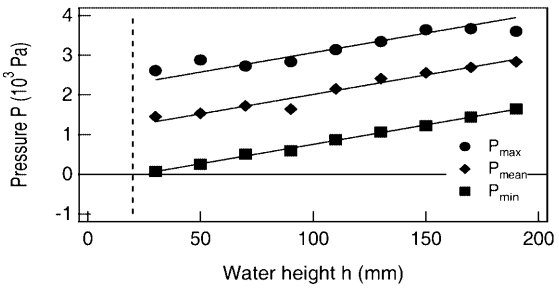

Fig. 3. Pressures P_{max}, P_{mean}, and P_{min} vs. water height h. The vertical line corresponds to the layer thickness s. ($D = 0.22$ mg/s, $s = 20$ mm, $d = 2$ mm, beads 225 μm)

3 Experimental results

The typical behavior of the pressure P as a function of time is shown in Fig. 2. The pressure increases almost linearly while the free surface is at rest and the gas trapped in the chamber (The non-linearity of the pressure increase is explained by a thermal effect, see Appendix). When the pressure reaches a threshold value P_{max}, a bubble of gas suddenly escapes through the granular layer, leading to a rapid pressure drop to P_{min}. One can notice that P_{min} is well defined and presents only little fluctuations that compare to the accuracy of pressure measurements. By contrast, P_{max} fluctuates by 10% around its mean value. The duration of the pressure drops from P_{max} to P_{min} is less than the characteristic time of the pressure transducer (about 0.1 ms). This part of the pressure signal cannot be described with our experimental setup. On the other hand, the characteristic time of the pressure increase is given by $(P_{max} - P_{min})/D$ and imposes the periodicity of the phenomenon. We point out, that the preparation procedure does not make possible to observe and analyze the first emission of gas. Moreover, on a long time period, much longer than the experimental times we are concerned with herein, the emission of bubbles leads to the formation of a crater. In the following, we give results obtained during the early steady regime, after emission of the first bubble, and before the deformation of the free surface is significant.

We measure systematically the minimum P_{min}, mean P_{mean}, and maximum P_{max} pressures during the first 120 seconds (Fig. 2). After each emission of gas, the pressure drops down to the same value P_{min}. We define P_{mean} as the mean value of the pressure over time. On the other hand, the pressure P_{max} is the absolute maximum value reached by the pressure during the acquisition time. We analyze, in the following, the influence of the experimental parameters d, h, s, D, V, and R on the pressure signal.

• The results do not depend, in any characteristics, on the diameter d of the hole in the range 1 to 3 mm. For large d, the small glass beads can flow down to the chamber, so that we limited our study to $d \leq 3$ mm. We choose the diameter of the hole larger than the characteristic size of the beads so as to insure that the formation of the bubble is not limited by the hole itself.

• The water level h only shifts the value of the pressure, according to the hydrostatics (Fig. 3): The slope of the linear interpolation of each of the pressures versus height h (e.g. 9.81 10^3 Pa/m) corresponds to the static variation of pressure in water at rest. In the following, we denote P^0_{max} and P^0_{min}, the maximal and minimal pressures estimated for $h = s$. This case corresponds to an immersed granular layer, the thickness of the water layer on top of it being zeroed. We already notice, that the minimum pressure $P^0_{min} \simeq 0$ in all our experimental conditions.

• The maximal pressure P^0_{max} does not depend on the granular layer thickness s (Fig. 4). This result holds true as long as $s \leq 50$ mm, while the diameter of the container is 90 mm. We decreased the diameter of the container, and checked that P^0_{max} is unchanged as long as s remains smaller than the radius of the cylinder. When the layer is thick, a large amount of gas can form a bubble trapped in the granular material which is then globally lifted. In the following, we exclude these finite-size effects by limiting our study to thin layers (i.e. smaller than 50 mm).

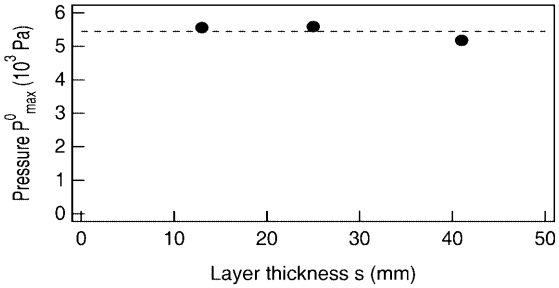

Fig. 4. Maximum pressure P^0_{max} vs. layer thickness s ($D = 0.22$ mg/s, $h = 100$ mm, $d = 2$ mm, beads 112 μm)

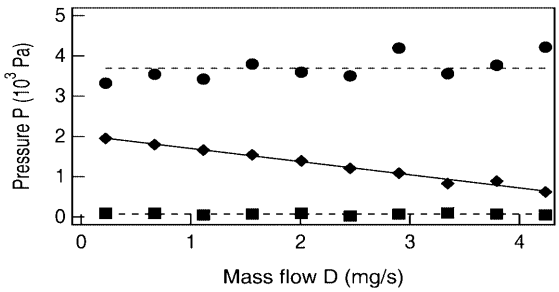

Fig. 5. Pressures P^0_{max}, P^0_{mean} and P^0_{min} vs. mass flow D ($h = 100$ mm, $d = 1$ mm, $s = 25$ mm, beads 225 μm)

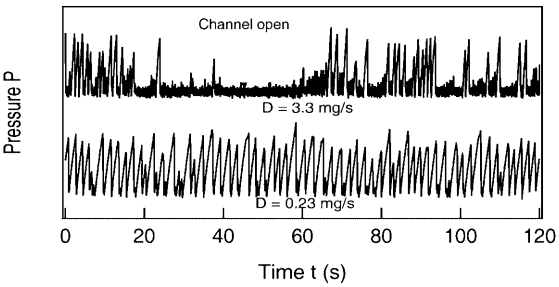

Fig. 6. Pressure P vs. time t. The pressure signals have been arbitrary shifted in the sake for clarity ($h = 100$ mm, $d = 1$ mm, $s = 25$ mm, beads 225 μm)

• The maximum pressure P^0_{max} does not depend on the mass flow D in the whole accessible range (0.2 to 4.3 mg/s, Fig. 5). On the other hand, the mean value of the pressure over time P_{mean} decreases linearly when D is increased. For large D, the pressure signal looses the periodicity that we observe for small mass flows (Fig. 6); The pressure signal presents two different types of pattern. One of them is composed of more or less regular successions of pressure increases and drops between P_{min} and P_{max} which correspond to emissions of distinct bubbles. By contrast, for significant periods of time, the pressure fluctuates close to its minimum value P_{min}. Bursts of small bubbles are then emitted through the granular layer. The duration of these bursts increases with the mass flow D, leading to the observed decrease of P_{mean}. One can then define a threshold value of D above which P_{mean} is expected to be zeroed (For instance, $D = 6.2$ mg/s, for $h = 100$ mm, $d = 1$ mm, $s = 25$ mm, beads 225 μm, Fig. 6).

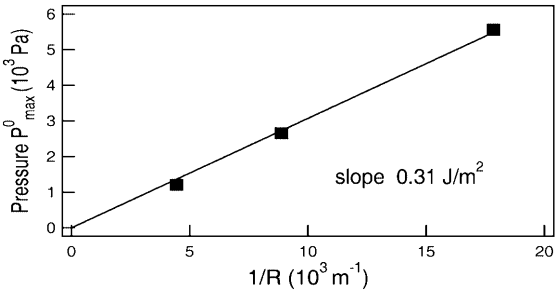

Fig. 7. Maximum pressure P^0_{max} vs. $1/R$. ($D = 0.22$ mg/s, $d = 2$ mm, $s = 20$ mm)

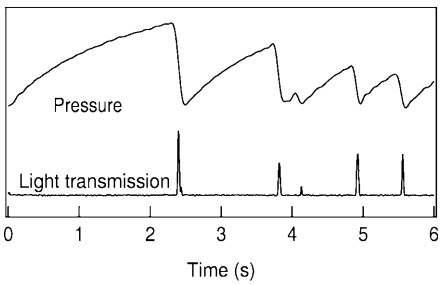

Fig. 8. Pressure and light transmission vs. time (arbitrary units). Each of the pressure drops corresponds to a sudden increase in the light transmission

• The maximum pressure P^0_{max} does not depend on the volume of the chamber V. A decrease of the volume of the chamber V has, qualitatively, the same effect as an increase of the mass flow D. The study of the dynamical regimes as functions of the mass flow D and volume V will be the subject of a further publication [5].

• At last, the maximum pressure P^0_{max} is proportional to $1/R$ where R is the radius of the glass-beads (Fig. 7). This dependance shows that the passage of the gas through the layer is not limited by its ability to move large groups of grains but by the possibility to form of a bubble in the void space between the grains.

4 Analysis

In the following, we discuss the forecoming experimental results and perform additional experiments in order to check the validity of our first conclusions.

We placed a light source underneath and a photodiode on top of the layer, and observed that a channel extends along the whole thickness of the granular layer during the gas emission. Indeed, the light transmission presents a maximum for each of the pressure drops (Fig. 8).

In order to visualize the channel, we reproduced the same experiment using a 2D vertical granular layer: The mixture of grains and liquid in sandwiched between two vertical glass plates (gap 2 mm). Air is injected at the bottom, through a 2 mm-in-diameter tube which is connected to an external chamber. The evolution of the pressure as a function of time is similar to the pressure signal given in Fig. 2. We show in Fig. 9 a picture of the granular layer

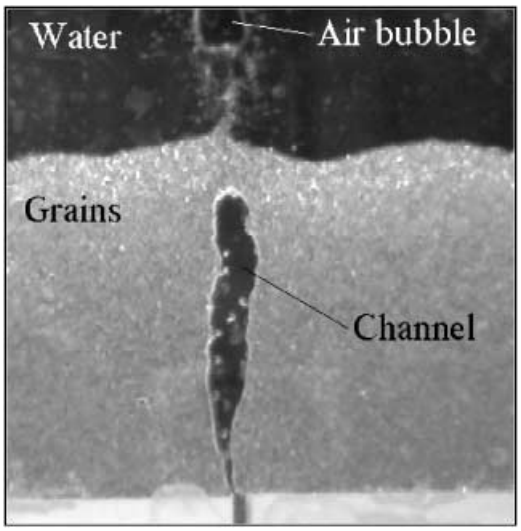

Fig. 9. Channel in a 2D experiment. The picture is taken at intermediate time between two bubble-emissions

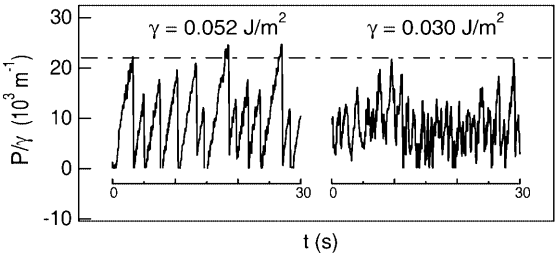

Fig. 10. Pressure P vs. time t. The pressure signal is normalized by the surface free energy γ. The decrease in γ is obtained by adding soap to water. The renormalized maxima of the pressure signal are not changed when soap is introduced in the system ($D = 0.22$ mg/s, $d = 2$ mm, $s = 20$ mm, beads 500 μm)

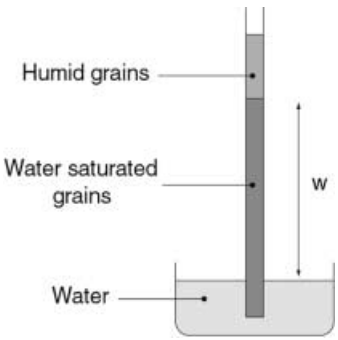

Fig. 11. Measurement of P^0_{max} in a vertical tube. The tube is filled with dry granular material and tapped. Water is poured from the top, and we measure the water height w at equilibrium which relates to P^0_{max} by $P^0_{max} = w\rho g$ ($\rho = 10^3$ Kg/m^3 is the specific mass of water and $g = 9.8$ m/s^2 the intensity of gravity). We find, for instance, $w = 13.2$ cm (resp. $w = 28.0$ cm) with 500 μm (resp. 250 μm) glass beads leading to $\Re = 0.31R$ (resp. $\Re = 0.30R$). In this case, the granular material is compact and the flow tends to increase the compaction: the grains can not move significantly. We measure the same ratio $\Re/R$ in both experiments. This is the experimental proof that P^0_{max} is reached when the granular packing, that forms the blockage, reaches its maximum compacity

right after a bubble emission: The channel almost extends over the whole thickness of the layer, and is sealed by a typical blockage at the top. In order to go through the layer, the gas creates a channel along the whole thickness of the sample. After emission of a bubble, only a small amount of granular material (typical size 10 bead-diameters) at the upper end of the channel collapses and forms a blockage that seals the system.

The upper part of the channel collapses as soon as the pressure in air becomes smaller than the pressure in water in this region: Water then tends to flow backwards inside the channel and helps the grains to fall down and to form the blockage. The minimal pressure P^0_{min} (Fig. 3) corresponds to the pressure difference between air and water at the free surface of the granular layer when the channel closes, and the value $P^0_{min} \simeq 0$ is not surprizing.

The creation of the channel can not account by itself for the value of the maximum pressure P^0_{max} which corresponds to the overpressure that makes possible to overcome the blockage. The linear interpolation of P^0_{max} as a function of $1/R$ leads to:

$$P^0_{max} = \frac{\alpha}{R} \tag{1}$$

with $\alpha = 0.31$ J/m^2. The overpressure P^0_{max} relates to the radius of curvature $\Re$ of the air-water interface by Laplace relation:

$$P^0_{max} = \frac{2\gamma}{\Re} \tag{2}$$

where γ is the surface free energy. We deduce from Eq. 1 and Eq. 2, $\Re \simeq 0.3R$ with $\gamma = 0.05$ J/m^2. In addition, one can check experimentally that the overpressure P^0_{max} is proportional to the surface free energy γ (Fig. 10) [6].

The overpressure P^0_{max} is simply given by Laplace relation involving the surface free energy of the liquid-air interface and the size of the grains. This is the experimental proof that the grains that seal the channel are not globally lifted. The passage of the gas is limited by the creation of a path in the narrow space between three grains at contact. This physical process explains why only the absolute maximum value of the overpressure P^0_{max} is reproducible: The compacity of the granular material that forms the blockage can be different after each bubble emission. The absolute maximum value P^0_{max} is then reached only if the granular material in the blockage reaches its maximum compacity [We performed, in addition, another simple experiment (Fig. 11), and checked that the experimental value of P^0_{max} that we measure, really corresponds to the overpressure that allow a gas to pass through a compact granular packing]. In order to overcome the blockage, the gas initially creates a path between the grains that do not move significantly during this process. The granular material is advected by the flow afterwards.

5 Conclusion

We studied experimentally the ability of air to locally pass through a thin immersed layer of granular matter. We

have shown that the gas creates, while passing through the layer, a channel that does not collapse after emission of a bubble; only a small amount of grains forms a blockage (typical size 10 bead diameters) that seals the channel at its upper end. The gas escapes the system when the pressure is enough to create a path between the grains. The grains do not move during this initial process, and the granular material is only advected later by the flows of air and water. Dependance of the threshold pressure on the grain size as well as on the surface free energy of the liquid-gas interface have been analyzed.

We plan to extend this work in three different directions: We will study in details the dynamical behavior of the pressure as a function of the volume of the chamber and of the air mass flow [5], and analyze the transition from the *periodic* regime (emission of distinct bubbles) to the *continuous* regime (continuous emission of gas). The long-term deformation of the free surface induced by the repetitive emission of gas and the formation of the crater will also be described experimentally. At last, we plan to extend our results to the limit where the diameter of the container is no more much larger than the thickness of the layer. This last experiment could help understanding the physics of explosive volcanoes as the material in the magmatic chamber where gas collapses is made of a mixture of a fluid (magma) and grains (rocks) [7].

Appendix

The increase of the pressure from P_{min} to P_{max} is expected to be linear in time as the mass flow is constant and the volume fixed when the gas is trapped in the chamber. The non-linearity observed experimentally (Fig. 2) is intriguing at first sight. Nevertheless, we show, in this appendix, that the sudden emission of one bubble leads to a cooling of the gas in the chamber that accounts for the experimental observations.

The emission of one bubble leads to a rapid pressure drop from P_{max} to P_{min}. The adiabatic expansion of air in the chamber leads to the temperature decrease ΔT which satisfies:

$$\frac{\Delta T}{T} = \frac{\eta - 1}{\eta} \frac{P_{max} - P_{min}}{P} \tag{3}$$

with $\eta \simeq 1.4$, the isentropic coefficient for a diatomic ideal gas (air). When the pressure reaches its minimum value P_{min}, the air in the chamber is colder than the surrounding walls of the container that remained at room temperature T_0.

The temperature T of the gas, which is in contact with the walls, then increases exponentially

$$T(t) = T_0 - \Delta T \exp(-\frac{t}{\tau}) \tag{4}$$

and reaches the temperature T_0 with the characteristic time τ, which depends on the geometry of the chamber (We estimated, in addition, $\tau \simeq 2 - 4$ s). The volume of the system is constant, and the increase of the temperature would lead by itself to a total pressure variation $\Delta P \simeq 0.28\ (P_{max} - P_{min})$. Nevertheless, the mass flow

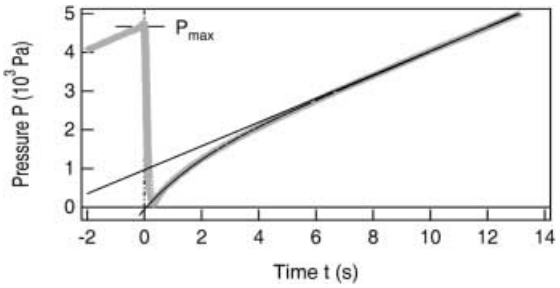

Fig. 12. Pressure P vs. time t. (Thick grey line: experimental data; Dash line: theoretical model; Plain line: asymptote.) We estimate $P_{max} - P_{min} = 4600$ Pa. The interpolation with Eq. 6 gives $\Delta P = 973$ Pa $\simeq 0.21(P_{max} - P_{min})$ with $\tau \simeq 3.4$ s. ($D = 0.22$ mg/s, $d = 2$ mm, $s = 25$ mm, beads 225 μm)

D of gas being kept constant, the mole number in the chamber increases with time and satisfies:

$$n(t) = n_0 + \frac{D}{M} t \tag{5}$$

where $M \simeq 29$ g is the molar mass of air and n_0 the mole number in the system right after the emission of the bubble. Thus, the variation of the pressure P as a function of time can be written, according to the state equation of the ideal gas,

$$\frac{P(t)}{P_0} = \Big(1 + \frac{D}{M n_0} t\Big)\left(1 - \frac{\eta - 1}{\eta} \frac{\Delta P}{P_0} \exp\Big(-\frac{t}{\tau}\Big)\right) . \tag{6}$$

The experimental data are in quantitative agreement with Eq. 6 (Fig. 12). Thus, the variations of the temperature of the gas in the chamber account for the non-linearity of the pressure increase observed experimentally.

References

1. J. Duran in *Sands, Powders, and Grains: An introduction to the physics of granular materials*, Springer-Verlag, New-York, 2000; G. H. Ristow in *Pattern Formation in Granular Materials*, Springer-Verlag, New-York, 2000
2. R. A. Bagnold, "Motion of waves in shallow water. Interaction between waves and sand bottoms" in *The physics of sediment transport by wind and water*, edited by C. R. Throne, R. C. MacArthur, and J. B. Bradley (American Society of Civil Engineers, New-York, 1988)
3. B. N. J. Persson in *Solid Friction*, Springer, New-York (1998); S. Nasuno, A. Kudrolli, and J. P. Gollub, Phys. Rev. Lett. **79**, 949 (1998); J.-C. Geminard, W. Losert, and J. P. Gollub, Phys. Rev. E **59**, 5881 (1999)
4. H. M. Jaeger, S. R. Nagel, and R. P. Behringer, Rev. Mod. Phys. **68** 1259 (1996)
5. The volume of the chamber V controls the stiffness of the system, while the ratio V/D imposes a characteristic time. We plan to study the state diagram in the plane (D,V) like already done in the plane (k: spring stiffness, v: driving velocity) in sliding friction [3]

6. We also increased the wettability of the glass surface, by cleaning the grains in sulfochromic acid, and obtained, in the case of perfect wetting (α =0), $\Re = 0.31R$. We had previously measured $\Re = 0.33R$ with the value $\theta \simeq 30$ deg of the contact angle and with the same value of the surface free energy γ. Thus, the overpressure P^0_{max} increases with the wetting. Nevertheless, we did not succeed in increasing the contact angle without modifying γ, and consider that the results are not accurate enough to be reliable
7. M. Ripepe, S. Ciliberto, and M. Della Schiava, J. of Geophys. Res. **106** 8713 (2001)